Fusion Engineering and Design 84 (2009) 867–874

Contents lists available at ScienceDirect

Fusion Engineering and Design

journal homepage: www.elsevier.com/locate/fusengdes

Plasma control system for "Day-One" operation of KSTAR tokamak

Sang-hee Hahn[a,*], M.L. Walker[b], Kukhee Kim[a], H.S. Ahn[c], B.G. Penaflor[b], D.A. Piglowski[b], R.D. Johnson[b], Jaehoon Choi[a], Dong-keun Lee[a], Jayhyun Kim[a], S.W. Yoon[a], Seong-Heon Seo[a], H.T. Kim[a], K.P. Kim[a], T.G. Lee[a], M.K. Park[a], J.G. Bak[a], S.G. Lee[a], Y.U. Nam[a], N.W. Eidietis[b], J.A. Leuer[b], A.W. Hyatt[b], G.L. Jackson[b], D. Mueller[d], A.S. Welander[b], G. Abla[b], D.A. Humphreys[b], W.C. Kim[a], Yeong-Kook Oh[a]

[a] National Fusion Research Institute (NFRI), Daejeon 305-333, Republic of Korea
[b] General Atomics, P.O. Box 85608, San Diego, CA 92186-5608, USA
[c] POSCON Corporation R&D Center, 101 Korea Techno Complex Building, Korea University, Seoul 136-713, Republic of Korea
[d] Princeton Plasma Physics Laboratory, NJ, USA

ARTICLE INFO

Article history:
Available online 30 January 2009

Keywords:
Tokamak
Plasma control
Poloidal field coil
Real-time control
Power supply control

ABSTRACT

A complete plasma control system (PCS) has been developed for KSTAR's first plasma campaign as a collaborative project with the DIII-D team. The KSTAR real time plasma control system is based on a conceptual design by Jhang and Choi [Hogun Jhang, I.S. Choi, Fusion Engineering and Design 73 (2005) 35–49] and consists of a fast real-time computer/communication cluster and software derived from the GA-PCS [Penaflor, B.G., et.al., Fusion Engineering and Design, 83 (2) (2008) 176]. The system has been used for simulation testing, poloidal field (PF) coil power supply commissioning and first plasma control.

The seven sets of up-down symmetric, superconducting PF coil/power supply systems have been successfully tested. Reflective memory (RFM) is utilized as the primary actuator/PCS real-time communication layer and PCS synchronization with KSTAR timing system and slower control devices is achieved through an EPICS implementation. Consistent feedback loop times of 100 microseconds has been achieved during PF coil power supply testing and first plasma commissioning. Here we present the "Day-One" plasma control system in its final form for the first plasma experimental campaign of KSTAR and describe how the system has been utilized during magnet commissioning and plasma startup experiments.

1. Introduction

The KSTAR (Korea Superconducting Tokamak and Advanced Research) [1–3] project has completed its construction of the main tokamak device in its startup configuration and launched the first coil Commissioning at May 2008. As a part of the KSTAR discharge control system [4], the plasma control system (PCS) provides real-time controllability, creating and sustaining plasma during the experimental campaign. With software derived from the DIII-D PCS [5,6], a special adoption of original hardware for a few first real-time feedback control loops has been done with a newly designed communication layer for KSTAR.

This work describes the configuration of the plasma control system developed for "Day-One" plasma operation, and summarizes the major performances achieved in both the superconducting magnet commissioning and the first plasma experiments.

2. System hardware layout

The PCS hardware consists of three parts for a complete feedback loop: data acquisition of plasma information from the tokamak, the real-time CPU for feedback calculations, and communication interfaces with the actuators. Fig. 1 shows the hardware layout for "Day-One" system.

Adopting the original DIII-D PCS software but accepting the philosophy of the original conceptual design [7], the following new features specific to KSTAR has been implemented: (1) a special real-time data communication layer through for fast feedback, (2) employment of a full digital control interface for the set of 7 PF power supplies, and (3) integration between the KSTAR time-synchronization system and the EPICS (Experimental Physics and Industrial Control System) [8] software environments which now prevail through the entire KSTAR control system [9,10].

2.1. Data acquisition

Two kinds of plasma diagnostics were used for the first plasma control: 82 channels of magnetic diagnostics [11] and a single chan-

* Corresponding author. Tel.: +82 42 870 1615; fax: +82 42 870 1619.
E-mail address: hahn76@nfri.re.kr (S.-h. Hahn).

0920-3796/$ – see front matter © 2008 Elsevier B.V. All rights reserved.
doi:10.1016/j.fusengdes.2008.12.082

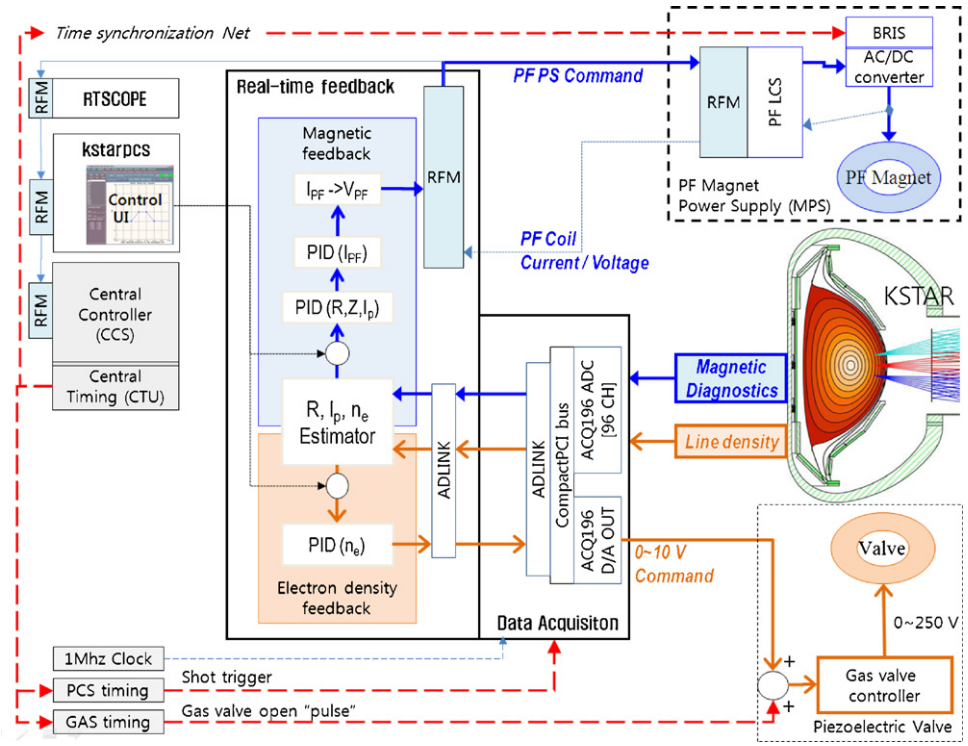

Fig. 1. The control system layout for the plasma control system (PCS) in Day-One configurations.

nel of the line-integrated electron density from millimeter-wave interferometer [12]. Differential analog cables were used to bring all raw voltage signals into the 96-channels D-TACQ ACQ196 [13] digitizer attached to the real-time CPU through a 66 MHz PXI-to-PCI link, providing 20 kS/s per channel. The 82 channels of magnetic diagnostics are splited through a panout box and collected by both the magnetics diagnostics acquisition system and the PCS digitizer. The attenuations for a 1 kHz, 100 mV square wave signal for the PCS acquisition system were within 0.1%. Table 1 summarizes the whole set of magnetic/plasma diagnostics collected for the PCS. An external clock source of 1 MHz has been used as a master clock for the digitizer and the real-time control part with 200 μs control cycle. Using a TTL-type trigger from the master timing synchronization system (TSS) [9], the PCS is synchronized to the KSTAR's master time clock within 1 μs.

2.2. Reflective memory cluster and digital communications

The real-time CPU part is an x86-based Linux cluster consisting of three Intel x86 servers, which are connected to each other by both a gigabit Ethernet and a shared memory card named reflective memory (RFM) [14]. Its high throughput, low latency, and hardware support for various form factors to connect different digital devices directly. Table 2 shows hardware specifications of the RFM. The RFM net supports a star-topology to minimize the number of hops for an RFM packet transfer. In the present configuration, the average hops between boxes is 4.

The master node, named kstarpcs, contains the main graphic user interface (GUI) application "Wave", communicates with the central controller (CCS) and assigns control input to the real-time CPU (RT-CPU) node for every shot. The RT-CPU node runs the real feedback loop under system-interrupt-free mode (RT-MODE) by a specialized Linux kernel [15] with the external clock from the PCS digitizer. In order to implement the RFM in this RT-MODE, a customized RFM device driver which enables reading/writing the reflective memory referred to PCI bus address without calling any system interrupts has been used [16]. For the first campaign, the third server box is dedicated to the real-time scope (RTSCOPE) of monitoring 4 selected signals during the shot [17], utilizing a 20 kbytes of RFM ring-buffer of 1 kHz samples. Fig. 2 shows the snapshot of the RTSCOPE application in 600-s operation of a single PF coil.

2.3. Actuator interfaces

The RFM network is mainly used for a digital communication structure between the PCS/PF magnet power supply (MPS). As

Table 1
Number of collected plasma diagnostics for possible "Day-One" real-time controls.

Diagnostics	No. of channels (with integrator)
Flux loop	5 (5)
Loop voltage	5 (–)
Magnetic pickup coil	42 (33)
Diamagnetic loop	2 (2)
Rogowski coil	3 (2)
Vessel current monitor	3 (2)
MM interferometer	1 (–)
Total	83 (44)

Table 2
Hardware specifications of reflective memory (RFM) card.

RFM parameters	Specifications
Average latency	0.4 μs per hop
Network speed	2.2 Gbaud/s
Throughput	174 MB/s
Required optics	LC duplex multimode 62.5/125 nm Up to ~300 m
Compatible form factors	VME, CompactPCI PMC, PCI
Memory per card	128 MB

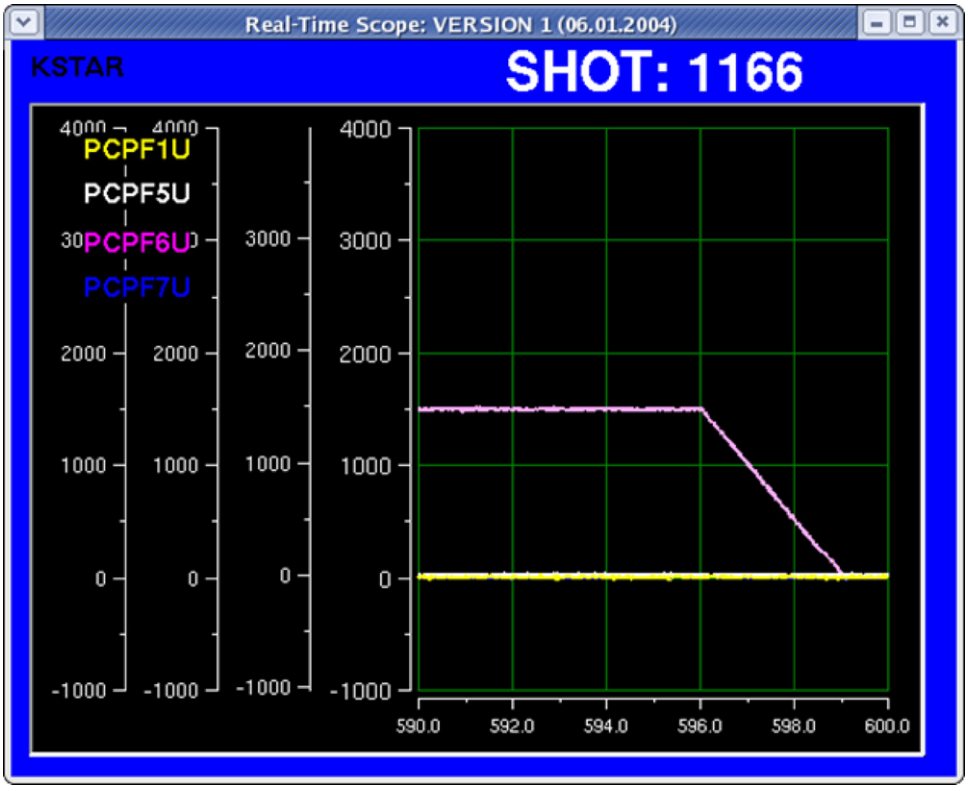

Fig. 2. A snapshot of real-time digital scope (RTSCOPE) utilizing RFM from a 10-min shot of the PF6 coil.

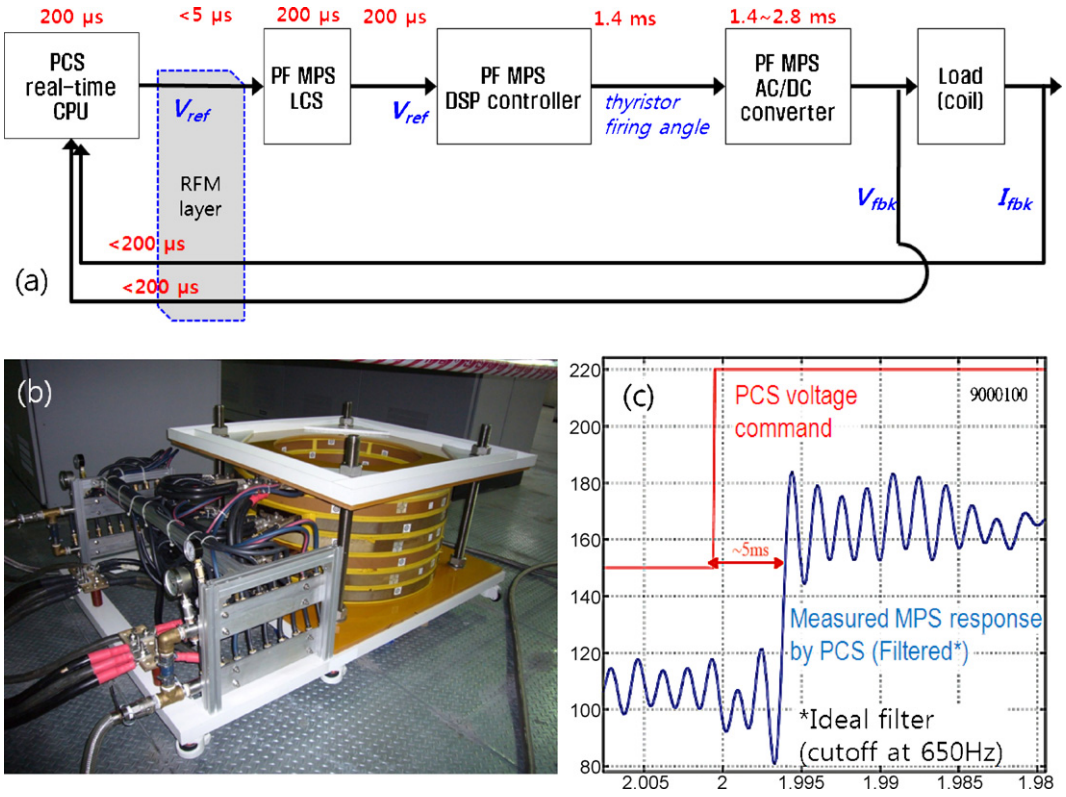

Fig. 3. (a) Communication scheme for coil current feedback between PCS/PF magnet power supply(MPS). (b) A high-inductance dummy load (29 mH, 50 m Ω) prepared for the PCS/PF MPS commissioning. (c) Voltage step response curve for a open-loop PCS voltage command on the dummy load. For blue signal an ideal low-pass filter at 650 Hz has been applied.

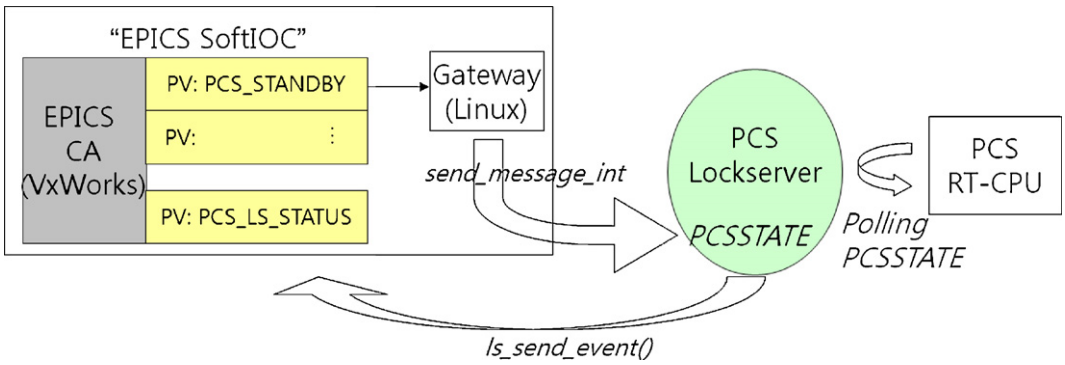

Fig. 4. Software PV integration scheme between the PCS state-machine ("lockserver") and the KSTAR central controller.

shown in Fig. 3(a), each MPS has a VME-based system called MPS local controller system (LCS). The LCS is connected to both the RFM network and the DSP controller, which calculates the thyristor firing angle for a 12-thyristor AC/DC converter according to the following formula:

$$\alpha = \cos^{-1}\left(\frac{V_{DC}}{1.35 \times V_{CMD}}\right), \quad (1)$$

where V_{DC} indicates maximum DC voltage of the PS and V_{CMD} denotes the command voltage from the PCS. Every 200 μs, the MPS LCS polls the PCS parameters and commands written to the RFM, sends them into the DSP, and uploads the measured MPS voltage and the coil current from the DSP into the designated RFM address so that the PCS can poll again. Each polling process costs communication delays of a half of inherent cycle time of each system (~100 μs) plus the time for updating the 10 kHz-sampled voltage measurement data from the DSP.

The PCS can choose either voltage command or current command mode as one of shot input parameters. In the *current command* mode, the PCS generates a coil current reference in real-time and the regulation of coil current is dealt by the inherent control logic of the DSP. In the *voltage command* mode, the PCS takes the feedback of the power supply and the DSP simply converts the command from the PCS into the thyristor firing angle by Eq. (1).

A software "echo" test was performed to verify the speed of communication by letting the DSP to return the same value to the address of "measured voltage" as soon as it received the voltage command from the PCS. The PCS collects both of them once at the end of the 50 μs fast cycle, and stores them separately into MDSplus [18]. The estimated and the measured (400–450 μs) are in agreement. System response was also measured using a high-inductance copper dummy shown in Fig. 3(b). As shown in Fig. 3(c), 5 ms of response delays in average was observed for a step voltage command of +70 V.

For the gas valve control, an analog 10 V-shielded BNC cable has been used to command the piezoelectric gas puff system [19] for real-time valve voltage control, using one of 16 channels of the D/A out panel from the acq196 digitizer. As shown in Fig. 1, the valve controller is manipulated by the *program* command signals from the PCS only when the gas timing *pulse* signal is at HIGH state to protect the valve in the unlikely events of the PCS remaining locked in the RT-MODE.

2.4. Integration and synchronization with central systems

For integration into the KSTAR shot sequence design, the PCS software has been modified to be able to utilize EPICS environment and functions dealing with the process variables (PV). Fig. 4 describes how the PCS state machine ("lockserver") communicates

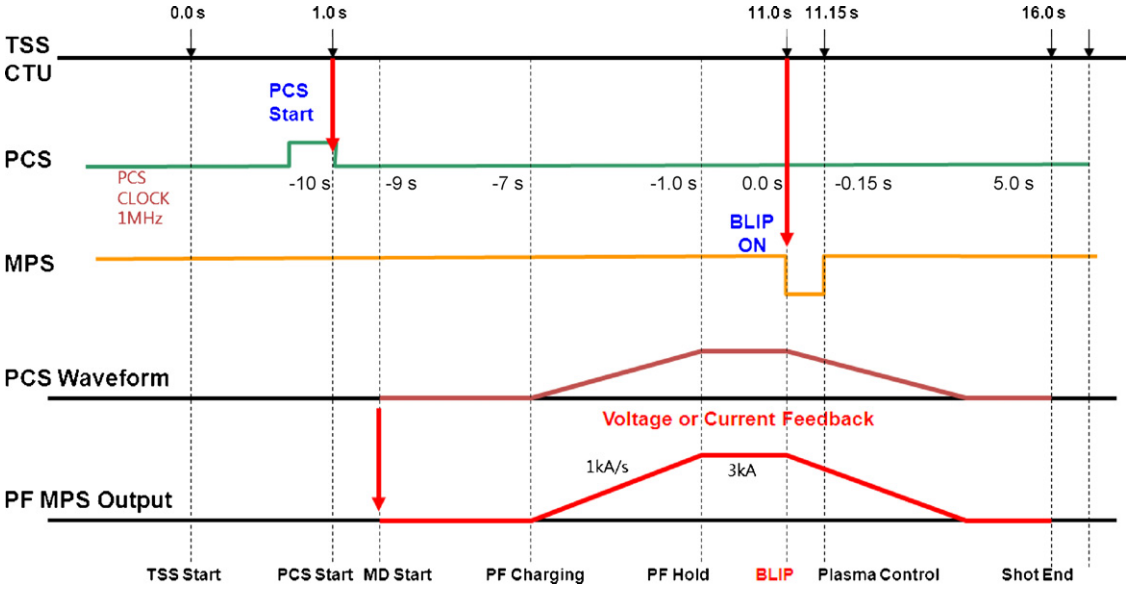

Fig. 5. Timing synchronization scheme for a PF magnet commissioning shot.

Table 3
Paramaters for the PF power supply system used in the first campaign.

PF MPS	Designed max voltages [V]	Designed U/D coil inductance [mH]	Blip resistor [Ω]
PF1	320	91.42	0.5
PF2	320	48.77	0.5
PF3	160	14.56	0.5
PF4	160	29.21	0.7
PF5	320	239.2	2.2
PF6	1000	450.9	2.1
PF7	1000	222.8	–

within the EPICS environment. A function running in the lockserver, *ls_send_event()*, updates a PV named PCS_LS_STATUS and enables the CCS to listen to the changes of the PCS_STATE. The CCS updates a PV named as PCS_STANDBY in a Linux-based gateway to the LOCKOUT state and the function *s* end_message_int sends a corresponding TCP/IP packet to the PCS to let it locked out.

Once the PCS is locked out and gets ready for a plasma shot, a "Shot Start" button from the CCS console enables the TSS to generate synchronized hardware triggers to various systems including diagnostics, the six sets of the blip resistor insertion system (BRIS), gas valve "pulse", and the electron cyclotron heating (ECH). The BRIS consists of a set of big resistors and a triggerable switch to provide a short, but fast flux swing on the superconducting PF coils during the breakdown/burnthrough phase of a plasma. During the first campaign, the BRIS can be activated for 100–150 ms. Fig. 5 shows an example of time synchronized shot sequence used for a PF magnet commissioning.

3. Applications to device commissioning and plasma experiments

3.1. Commissioning of PF magnets

Individual PF power supply was tested with a high-inductive dummy load for verifying digital feedback loop. After the cooldown, PI gain tuning of coil current on each up–down symmetric pair of PF coils and synchronization check with BRIS have been performed as one of prerequisites for the plasma operation. Table 3 summerizes the parameters of PF MPS used for first plasmas; hardware limit of PS voltage, optimized gain sets and the approximate resistance of the blip resistors.

The time synchronization of the blip resistor and the PCS has been measured in every shot by collecting the terminal-to-terminal voltage of the individual BRIS to the PCS. For the superconducting coil loads all the BRIS switch were activated within 100 μs jittering as shown in Fig. 6. Also the attempts for exerting additional power supply voltage, V_{PS}, during the BRIS activation were successful.

3.2. Plasma density feedback

The gas valve controllability has also been tested in the presence of magnetic field during the magnet commissioning and showed negligible difference from the one without any fields. A fringe-jump correction algorithm [20] on the millimeter-wave interferometer has been implemented into the PCS control loop for the line electron density estimation. The most accurate measurement is provided by Channel 1 among the 4 fringe outputs, which turned out to show no noise-induced fringe jumps. Based on this 10 kHz-sampled estimate, a PID controller for the line-averaged electron density has been utilized in several plasma shots. Fig. 7 summarizes the typical step response of the fuel and the density feedback result in a plasma shot. The density feedback algorithm in the PCS turned on at −50 ms with Gp = zero. After 50 ms from the BRIS start, the density feedback gain turned on as shown in Fig. 7. Experimentally, it took approximately 100 ms to make the density to a 90% of desired level.

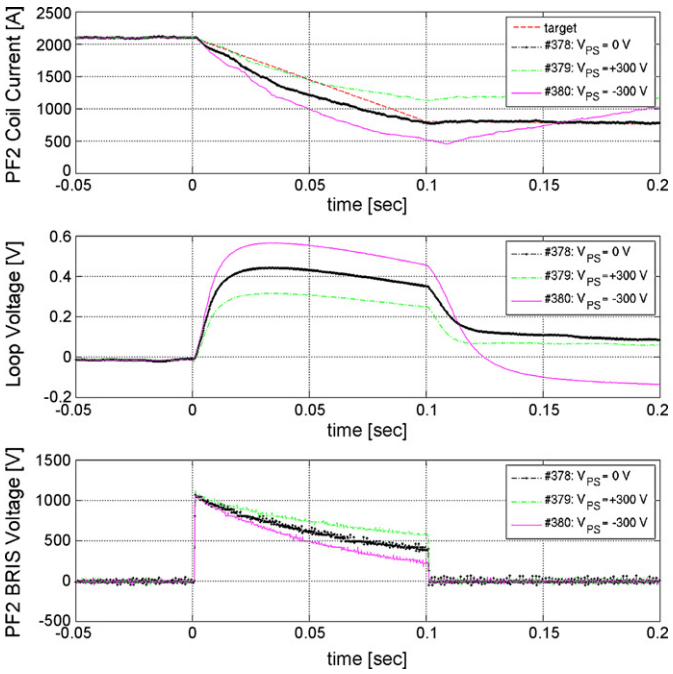

Fig. 6. Superconducting PF commissioning: BRIS activation test for PF2 coil. The coil current (above), the induced loop voltage at HFS midplane (middle) and the BRIS voltage measured at the blip period (below) are shown in the 3 cases of additional $V_{PS} = 0, \pm 300$ V.

3.3. Magnetic feedback controls

The breakdown of the first hydrogen plasma has been performed by providing complete feedforward set of seven coil current waveforms and a gas command with coil current feedback turned on. It took about 150 ms of simultaneous BRIS activations to raise plasma current over 100 kA level. After the BRIS ends, feedback of the

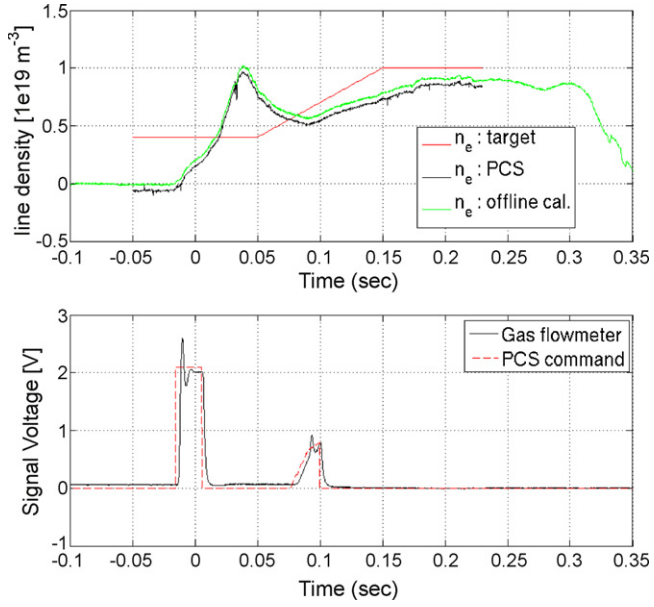

Fig. 7. Line-integrated density control result on shot 1001. The converted interferometer signals (top) on the PCS and the offline calculation reference. The PCS commands (bottom) were limited to 3 V and the feedback gain was set to Gp = 5.0.

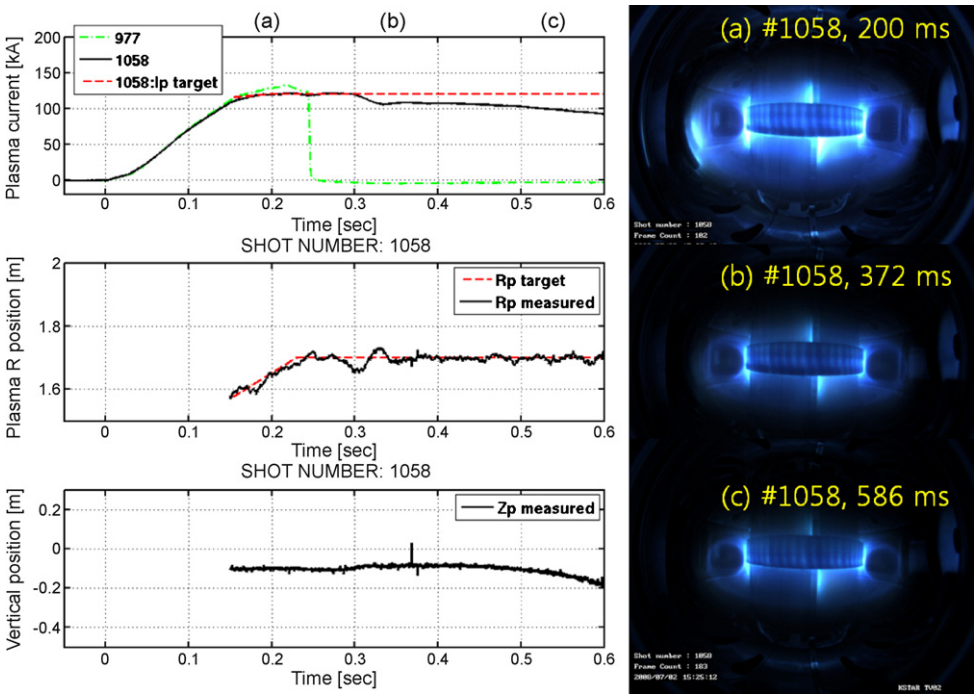

Fig. 8. Utilizing plasma control: a shot without any feedback (shot 977) and the other with I_p and R_p controls set on at $t = 150$ ms (shot 1058). The camera figure represents (a) ECH is still active (b) after the ECH turned off and (c) onset of vertical displacement event (VDE) as the plasma gets cold and shrinks.

plasma radial position R_p and the plasma current I_p starts. Since the magnetic coil geometry is up-down symmetric, vertical position is inherently close to $Z = 0$ and not controllable.

In order to measure the plasma major radius, 2 pairs of tangential B-probes at ±6 cm the inner/outer midplane were used to get the linearized largest plasma response for R_p estimator normalized to I_p. The vessel contribution was not considered. The vertical position, Z_p, also has been measured separately using another 5 pairs of the tangential probes.

Effects of the plasma feedback controls are shown in Fig. 8. The two shots, 977 and 1058, have the same breakdown scenario of 0.9 Webers until 150 ms. In shot 1058, control algorithm for

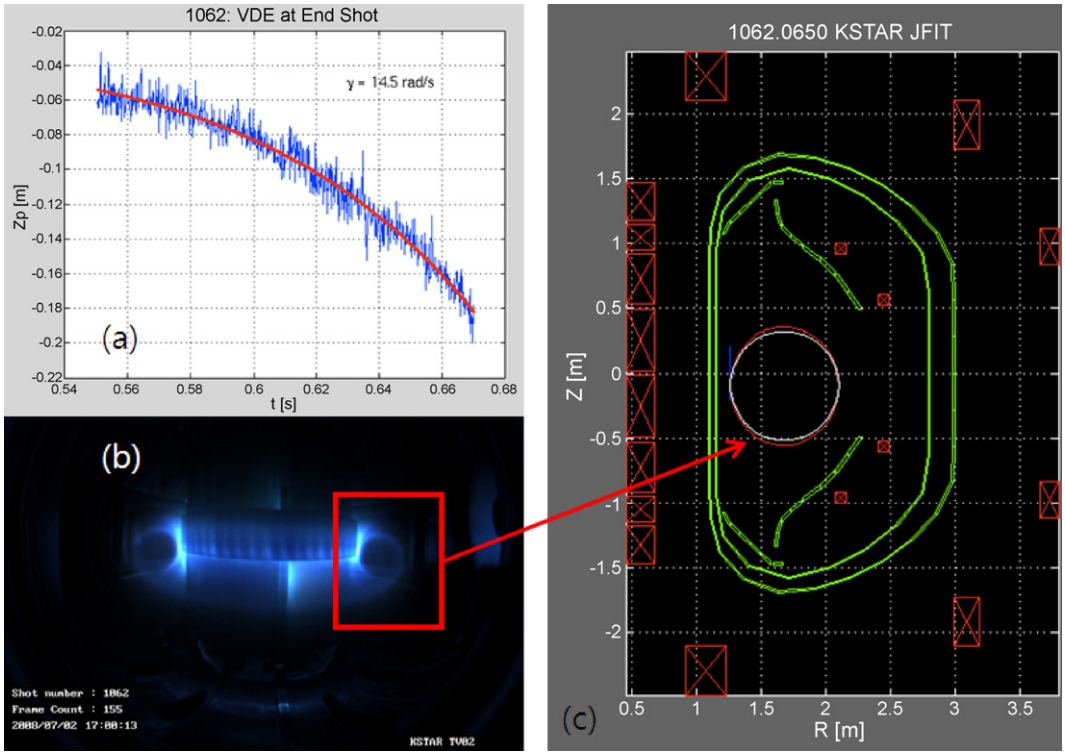

Fig. 9. Example of onset of a VDE (a) the growth rate, compared with the actual Z_p measured in shot 1062. (b) The camera image shows the plasma start to descend and deforms vertically, which is also seen in (c) JFIT reconstruction at 650 ms showing elongation.

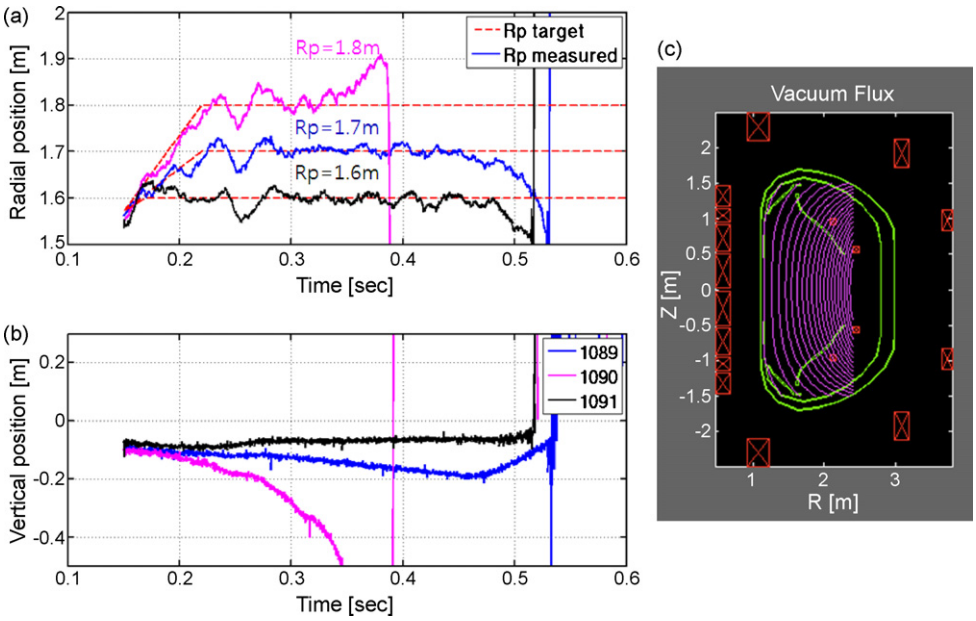

Fig. 10. Varying plasma radial positions: (a) At $R_p > 1.8$ m the VDE onset is much faster than the others. (b) The time variation of plasma vertical position. (c) The "concave" vacuum flux profile shown in JFIT reconstruction.

R_p and I_p is turned on at 150 ms. As a result, the plasma is sustained over 720 ms and maintains over 100 kA for 384 ms with 125 Hz-modulated 330 kW ECH pulse lasting until $t = 300$ ms. The excursion of R_p was within ± 3 cm and the largest one occurred when the ECH power was turned off and the plasma shrunk as seen in Fig. 8(b), accompanied with a little I_p drop. The validity of Z_p estimate has been confirmed by a 200 frames/s CCD camera shown in Fig. 8(c). This VDE occurs almost in every shot, when the plasma gets cold and shrinks. Regardless of the growth direction, the fitted VDE growth rate of 14.3 ± 0.2 rad/s is matched well to the experiment as shown in Fig. 9(a). The plasma deformation has been observed in Fig. 9(b), which matches in JFIT [21] reconstructions at 650 ms in Fig. 9(c), where we can see the vertical field stretches the plasma to the elongation of 1.1.

As shown in Fig. 10, control experiments with varying R_p were performed as a part of sawtooth activity measurements. With the ECH lasting until 240 ms, the plasma pushed to the outboard region suffered strong vertical instability and crashed to the vertical wall. From the concave PF field in outboard side shown in Fig. 10(c), it is apparent the unfavored field index outboard makes the plasma column vulnerable to VDE. Experiments showed that the marginally stable radial position is about at $R_p = 1.75$ m.

Exploitations to the longer plasma pulses was performed by moving the plasma column to the inboard side, as shown in Fig. 11. Basically it reduced the plasma volume and minimized the volt-second consumptions to sustain the plasma in the same I_p level, showing minimal corrosion effects due to the plasma crash to the first wall. In comparison with constant R_p case, the plasma followed the feedback and lasted to 746 ms. Also maximum available ohmic Webers was tried, expanding the pulse just only 100 ms. It is very difficult to estimate the plasma power balance quantitatively with no radiation measurements and unknown wall conditions, however it is reasonable to think that the way of activating BRIS to create a loop voltage always leaves a fixed percentage of the remaining coil flux, hence merely raising the maximum Webers would have limitations. The longest pulse of a plasma was approximately 866 ms with 1.1 Webers of total PF flux.

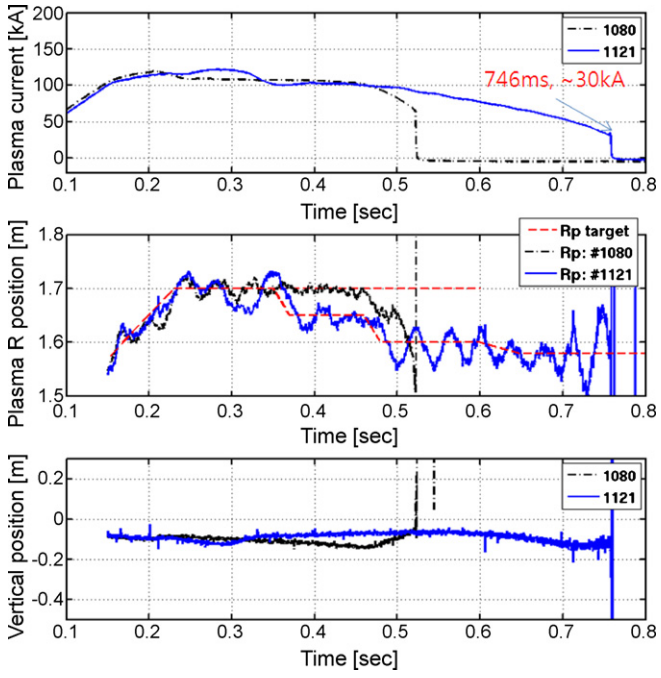

Fig. 11. Longer pulse exploitation by magnetic feedback. To avoid unfavored curvature outside the plasma is pushed into the inboard side from 1.7 to 1.6 m in the shot 1121. Comparisons of constant R_p case is also shown.

4. Conclusion and future work

A plasma control system (PCS) for "Day-One" operation of KSTAR tokamak has been developed as a form of reflective memory (RFM) cluster based on the Linux X86 architecture and the DIII-D PCS software. The cluster with a single real-time control node, seven sets of up–down symmetric PF coil/power supply system and a piezoelectric gas valve has been installed completely and operated through both the PF coil commissioning and the first KSTAR plasma campaign without any serious system problem. Utilization of the PCS magnetic feedback on the plasma current and position for a limited circular plasma enabled longer pulses and therefore observations of some interesting physical phenomena.

Acknowledgment

This work has been supported by the US-KSTAR collaboration program of US Department of Energy (DoE), and by Korea Ministry of Education, Science and Technology.

References

[1] G.S. Lee, J. Kim, S.M. Hwang, C.S. Chang, H.Y. Chang, M.H. Cho, et al., The KSTAR project: an advanced steady state superconducting tokamak experiment, Nuclear Fusion 40 (3y) (2000) 575–582.
[2] J.S. Bak, C.H. Choi, H.L. Yang, J.W. Sa, H.K. Kim, B.C. Kim, et al., Key features and engineering progress of the KSTAR tokamak, IEEE Transactions on Plasma Science 32 (2004) 757.
[3] Y.K. Oh, H.L. Yang, Y.S. Kim, K.R. Park, W.C. Kim, M.K. Park, et al., Completion of the KSTAR construction and its role as ITER pilot device, Fusion Engineering and Design 83 (2008) 804–809.
[4] K. Kim, M. Park, S.-h. Hahn, M. Kim, J. Hong, S. Baek, et al., Development and commissioning results of the KSTAR discharge control system, Fusion Engineering and Design 84 (2009) 1049–1054.
[5] B.G. Penaflor, J.R. Ferron, M.L. Walker, D.A. Humphreys, J.A. Leuer, D.A. Piglowski, et al., Worldwide collaborative efforts in plasma control software development, Fusion Engineering and Design 83 (2) (2008) 176.
[6] D.A. Piglowski, J.R. Ferron, P. Gohil, R.D. Johnson, B.G. Penaflor, et al., Enhancements in the second generation DIII-D digital plasma control system, Fusion Engineering and Design 81 (2007) 1058–1063.
[7] H. Jhang, I.S. Choi, Design concepts for KSTAR plasma control system, Fusion Engineering and Design 73 (2005) 35–49.
[8] EPICS homepage, http://www.aps.anl.gov/epics/.
[9] M.K. Park, Operation Results of KSTAR Integrated Control System for First Plasma, in: Proceedings of 22nd IAEA Fusion Energy Conference, 2008.
[10] K.H. Kim, C.S. Ju, M.K. Kim, M.K. Park, J.W. Choi, M.C. Kyum, The KSTAR integrated control system based on EPICS, Fusion Engineering and Design 81 (2006) 1829–1833.
[11] S.G. Lee, J.G. Bak, E.M. Ka, J.H. Kim, S.H. Hahn, Magnetic diagnostics for the first plasma operation in Korea superconducting Tokamak advanced research, Review of Scientific Instruments 79 (2008) 10F117.
[12] Y.U. Nam, M.S. Cheon, M. Kwon, Y.S. Hwang, Design of a single-channel millimeter-wave interferometer system for KSTAR, Review of Scientific Instruments 74 (3) (2003) 1613.
[13] http://d-tacq.com/acq196cpci.shtml.
[14] GE Fanuc homepage, http://www.gefanucembedded.com.
[15] B.G. Penaflor, J.R. Ferron, D.A. Piglowski, R.D. Johnson, M.L. Walker, Real-time data acquisition and feedback control using Linux Intel computers, Fusion Engineering and Design 81 (15–17) (2006) 1923–1926.
[16] Seong-Heon Seo, Performance test of the reflective memory based plasma control system, Presentation for the 6th IAEA TM on Control, Data Acquisition, Remote Participation for Fusion Research, P1-41, June 2007.
[17] Sang-hee. Hahn, Recent Progress of the KSTAR Plasma Control System, in: Proceedings of the 5th IAEA TM on Steady State Operation of Magnetic Fusion Devices, Daejeon, Korea, 2007.
[18] MDSplus Homepage, http://www.mdsplus.org.
[19] Seong-Heon Seo, H.t. Kim, K.P. Kim, Y.O. Kim, W.C. Kim, H.L. Yang, et al., Korea superconducting tokamak advanced research vacuum and gas puffing system, Review of Scientific Instruments 79 (2008) 116103.
[20] Y.U. Nam, Multi-fringe counting technique of millimeter-wave interferometer system for KSTAR, Presentation on the 7th International Conference on Open Magnetic System for Plasma Confinement, July 2008.
[21] D.A. Humphreys, A.G. Kellman, Analytic modeling of axisymmetric disruption halo currents, Physics of Plasmas 6 (7) (1999) 2742–2756.